Bioorganic & Medicinal Chemistry 19 (2011) 7482–7492

Contents lists available at SciVerse ScienceDirect

Bioorganic & Medicinal Chemistry

journal homepage: www.elsevier.com/locate/bmc

Time-dependent slowly-reversible inhibition of monoamine oxidase A by N-substituted 1,2,3,6-tetrahydropyridines

Wisut Wichitnithad [a,b], James P. O'Callaghan [c], Diane B. Miller [c], Brian C. Train [a], Patrick S. Callery [a,*]

[a] Department of Basic Pharmaceutical Sciences and Mary Babb Randolph Cancer Center, West Virginia University, Morgantown, WV 26506, USA
[b] Department of Pharmaceutical Technology (International Program), Chulalongkorn University, Bangkok 10330, Thailand
[c] Centers for Disease Control and Prevention, National Institute for Occupational Safety and Health, Morgantown, WV 26506, USA

ARTICLE INFO

Article history:
Received 1 August 2011
Revised 6 October 2011
Accepted 14 October 2011
Available online 21 October 2011

Keywords:
Tetrahydropyridine
Monoamine oxidase
Time-dependent inhibition
Covalent
Sodium borohydride

ABSTRACT

A novel class of N-substituted tetrahydropyridine derivatives was found to have multiple kinetic mechanisms of monoamine oxidase A inhibition. Eleven structurally similar tetrahydropyridine derivatives were synthesized and evaluated as inhibitors of MAO-A and MAO-B. The most potent MAO-A inhibitor in the series, 2,4-dichlorophenoxypropyl analog **12**, displayed time-dependent mixed noncompetitive inhibition. The inhibition was reversed by dialysis, indicating reversible enzyme inhibition. Evidence that the slow-binding inhibition of MAO-A with **12** involves a covalent bond was gained from stabilizing a covalent reversible intermediate product by reduction with sodium borohydride. The reduced enzyme complex was not reversible by dialysis. The results are consistent with slowly reversible, mechanism-based inhibition. Two tetrahydropyridine analogs that selectively inhibited MAO-A were characterized by kinetic mechanisms differing from the kinetic mechanism of **12**. As reversible inhibitors of MAO-A, tetrahydropyridine analogs are at low risk of having an adverse effect of tyramine-induced hypertension.

1. Introduction

Monoamine oxidase (MAO, EC 1.4.3.4) is a flavoenzyme that catalyzes the deamination or dealkylation of a broad spectrum of biogenic and xenobiotic primary, secondary and tertiary arylalkylamines. MAO-A inhibitors have therapeutic utility for the treatment of depression and MAO-B inhibitors for the treatment of Parkinson's disease.[1,2] The first generation of MAO inhibitors irreversibly inhibited the enzyme. Adverse effects associated with irreversible inhibition have relegated MAO-A inhibitors to secondary importance as therapeutic agents. The most notable adverse effect is tyramine-induced hypertension known as the 'cheese effect'.[3] Newer generation MAO inhibitors reversibly inhibit the enzyme and are less likely to produce hypertension. Tight-binding reversible inhibitors of MAO-A that do not have the liability of tyramine potentiation provide a solid basis for a worthwhile drug discovery target.[1] MAO-A and MAO-B enzymes are flavoproteins that are similar in structure and appear to share the same catalytic mechanism.[4] Remarkable substrate selectivity has been achieved in MAO inhibitor drug discovery by taking advantage of subtle differences in MAO-A and MAO-B structure, such as the recognition that human MAO-A (hMAO-A) has a smaller hydrophobic active site than hMAO-B and that there are differences in allosterically regulated entrance cavity space.[5]

Irreversible MAO inhibitors are characterized by covalent adducts with enzyme resulting from bioactivation of the inhibitor to an electrophilic intermediate. In Scheme 1 are partial structures of covalent adducts that have been proposed to explain the mechanism of irreversible inhibition of MAO by bioactivated propargylamines,[6,7] cyclopropylamines,[8] and allylamine.[9] The identity of the enzyme-bound site trapped by the electrophilic metabolite has been proposed to be the *N*-(5)[6,7] or *C*-(4a)[10] position of the flavin cofactor or a nucleophilic residue distant from the catalytic site, such as a cysteine[8,11] or other nucleophilic amino acid.[12,13]

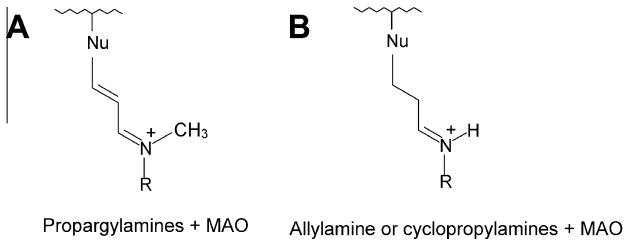

Scheme 1. Proposed partial structures of covalent intermediates in the inhibition of monoamine oxidase by (A) propargylamine inhibitors, such as clorgyline and rasagaline and (B) by allylamine or cyclopropylamines.

* Corresponding author. Tel.: +1 304 293 1482; fax: +1 304 293 2576.
E-mail address: pcallery@hsc.wvu.edu (P.S. Callery).

0968-0896/$ - see front matter © 2011 Elsevier Ltd. All rights reserved.
doi:10.1016/j.bmc.2011.10.038

The inhibitor binding site of MAO-A is formed by a hydrophobic cavity that extends from the flavin ring to a cavity-shaping 7-residue hydrophobic loop.[5] The closest enzyme nucleophile available to quench catalytically formed reactive intermediate electrophiles is the flavin moiety.[6,7,10] If the life-time of the electrophile is long enough to allow for exiting from the active site that is populated with residues of low nucelophilicity,[6] there are multiple nucleophilic cysteine residues accessible near the entrance to the catalytic site, as well as on the solvent accessible enzyme surface. MAO-A is known to be sensitive to thiol oxidation and thiol reagents.[14] Two cysteine residues (Cys-321 and Cys-323) are located near the entry to the catalytic site, although mutations in Cys-321 or Cys-323 do not influence catalytic activity.[15] On the other hand, when the surface cysteine Cys- 374 was mutated to alanine[8] or serine,[15] a significant decrease or loss of catalytic efficiency of MAO-A was observed. Time-dependent incorporation of multiple equivalents of allylamine was observed in MAO-B, most likely cysteines, indicates the potential for multiple contributing binding sites in addition to the flavin.[8,16]

Surface cysteines may play an allosteric role in regulating the active site conformation[8] leading to the suggestion that MAO-A activity can be modulated from the surface.[16] Kinetic studies have revealed allosteric binding sites in MAO-B. The high and low affinity imidazoline I_2 allosteric regulatory sites on MAO-B are consistent with inhibitor binding within the entrance channel of the enzyme.[17] Allosteric inhibition at I_2 sites is competitive for MAO-A and competitive, noncompetitive or mixed mechanisms on MAO-B.[18] There is crystal structure support for an allosteric mechanism involving imidazoline ligand binding in a binding site other than the catalytic site on MAO-B.[19]

The 1,2,3,6-tetrahydropyridine moiety is a scaffold in drug discovery efforts[20–23] and a contributing pharmacophore to the MAO-bioactivated neurotoxin precursor 1-methyl-4-phenyl-1,2,3,6-tetrahydropyridine (MPTP).[24] Thermally unstable piperidines, such as fentanyl are known to rearrange to form tetrahydropyridine degradation products.[25,26] Exposing fentanyl to high heat or electrospray ionization mass spectrometry causes a β-elimination reaction producing a tetrahydropyridine, 1-(2-phenylethyl)-1,2,3,6-tetrahydropyridine (**1**). Because of the structural similarity of **1** with known substrates and inhibitors of MAO, such as MPTP, several analogs of **1** were synthesized and evaluated for selective MAO inhibitory activity.

2. Results and discussion

2.1. Chemistry

Scheme 2 illustrates the synthetic pathway leading to N-substituted phenyl alkyl tetrahydropyridine analogs. *N*-alkylation of phenyl alkyl halides afforded the corresponding pyridinium salts. Reduction of the resulting pyridinium ions with sodium borohydride in protic solvent was a convenient way to generate *N*-phenylalkyl-1,2,3,6-tetrahydropyridines **1**–**9**. As proposed by Mabic et al.,[27] incorporation of a hydride from the reducing agent initially takes place at *C*-6. The resulting 5,6-dihydropyridine is then protonated at *C*-3 to yield the corresponding iminium conjugate acid. Subsequent reduction of the iminium ion yields N-substituted 1,2,3,6-tetrahydropyridines. Synthesis of the piperidyl analog **10** was accomplished through reductive alkylation of the iminium ion formed between phenyl acetaldehyde and piperidine using sodium borohydride. The 2,4-dichlorophenoxypropyl analog **12** was synthesized by reaction of 2,4-dichlorophenol with an excess of 1,3-dibromopropane in the presence of sodium hydride through intermediate **11**. *N*-Alkylation of **11** with pyridine yielded the corresponding pyridinium salt, which upon reduction with sodium borohydride gave **12**.

2.2. MAO inhibition

The tetrahydropyridine analogs inhibited human recombinant MAO-A at lower concentrations than required to inhibit MAO-B (Table 1). IC_{50} values for MAO-A inhibition were calculated to be in the low to middle μM range, whereas IC_{50} values for MAO-B were in the high μM to mM concentration range. An exception of MAO-A selectivity was the 4-methyl analog **9**, exhibiting the lowest potency and selectivity as an MAO-A inhibitor among the tetrahydropyridines screened. Although only one piperidine analog was evaluated, the contribution of unsaturation in the tetrahydropyridine ring to MAO inhibitory activity

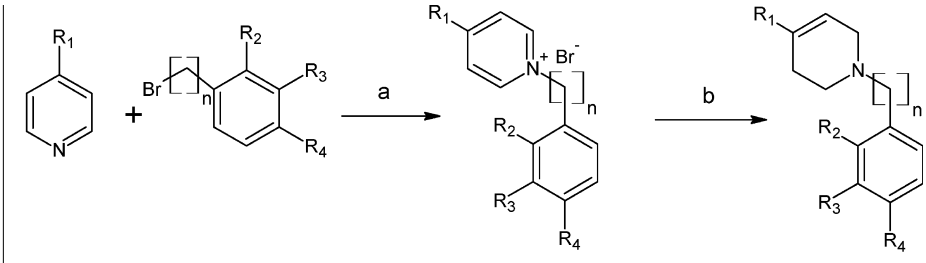

1-9

Compounds	n	R_1	R_2	R_3	R_4
1	2	H	H	H	H
2	2	H	H	H	F
3	2	H	H	H	CH_3O
4	2	H	H	CH_3O	CH_3O
5	3	H	H	H	H
6	2	H	Cl	H	Cl
7	2	H	H	H	NO_2
8	1	H	H	H	H
9	2	CH_3	H	H	H

Scheme 2. Preparation of N-substituted tetrahydropyridines **1**–**9**. [a]140 °C, 75–85% yield; [b]$NaBH_4$, MeOH, 0 °C, 70–89% yield.

was suggested by the observation of low MAO inhibitory potency of piperidine-containing **10**. Substitution on the phenyl ring of **1** produced analogs of varying potency, although all were selective for MAO-A. The chain length of one to three methylene groups separating the phenyl and tetrahydropyridine moieties slightly influenced both selectivity and potency. Compound **8**, with a side chain one methylene shorter than that of compound **1**, was less potent than **1,** but more selective for MAO-A. Extending the phenylethyl chain to phenylpropyl produced **5** with similar potency and selectivity as **1**.

Compound **12** is similar in structure to the selective MAO-A inhibitor clorgyline, differing in replacement of the propargyl group of clorgyline with a tetrahydropyridyl group. Compound **12** displayed the highest inhibitory potency in the series, placing this compound among the most MAO-A selective compounds of the synthesized tetrahydropyridine MAO inhibitors.

2.3. MAO-A enzyme kinetics

The kinetic profile of **1** was consistent with uncompetitive, reversible inhibition of human recombinant MAO-A, and was independent of preincubation time. In contrast, **12** inhibited MAO-A with a profile consistent with mechanism-based, time-dependent, covalent, slowly-reversible inhibition. Human recombinant MAO-A was incubated with kynuramine[28] as substrate in the absence and presence of inhibitors **1**, **9**, **10** and **12**. Several kinetic mechanisms were identified in the tetrahydropyridine series, including uncompetitive, mixed competitive, noncompetitive and time-dependent inhibition. For **1**, a Lineweaver–Burk reciprocal plot (Fig. 1A, upper panel) demonstrated that the inhibition of MAO-A was uncompetitive with an experimentally-derived K_i value of 9.2 ± 1.9 μM obtained from y-intercept replots (Fig. 1A, lower panel) exhibiting decreases in both K_m and V_{max} with increasing inhibitor concentration. IC_{50} values were also calculated using the Cheng–Prusoff[29] equation: $IC_{50} = K_i\ (1+K_m/S)$ for uncompetitive reversible inhibition. For compound **1**, the calculated IC_{50} (45.4 ± 4.5 μM) was found to be close to the experimental IC_{50} shown in Table 1 (41.3 ± 1.5 μM). For uncompetitive inhibitors, such as compound **1**, the Cheng–Prusoff equation indicates that the inhibitory effect of **1** depends on the substrate concentration. These results suggest the involvement of inhibitor binding at an allosteric site. Since a characteristic of uncompetitive inhibitors is

Table 1
Inhibitory effects of tetrahydropyridine analogs on recombinant human MAO-A and MAO-B

Compound	Structure	IC_{50} (μM) ±SD[a]		Selectivity index[b]
		MAO-A	MAO-B	
1	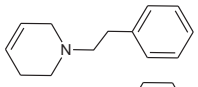	41.3 ± 1.5	1184.4 ± 9.9	28.7
2	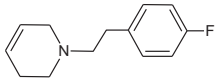	27.3 ± 1.3	5265.9 ± 10.9	192.6
3	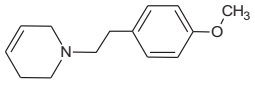	12.0 + 0.7	96.1 + 0.7	8.0
4	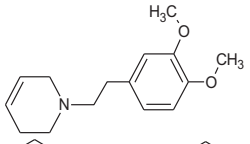	110.8 ± 2.4	1362.9 ± 32.9	12.3
5	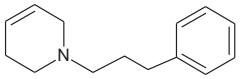	86.1 ± 0.58	812.5 ± 6.4	9.4
6	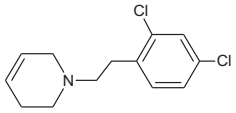	6.1 ± 0.04	67.2 ± 2.4	11.1
7	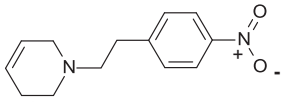	37.8 ± 0.6	271.9 ± 3.5	7.2
8	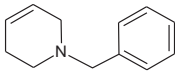	157.1 ± 4.4	6536.8 ± 102.5	41.6
9	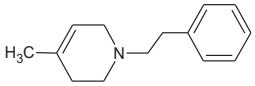	623.4 ± 2.0	1245.1 ± 14.7	2.0
10	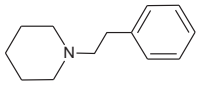	757.3 ± 4.5	761.5 ± 11.2	1.0
12	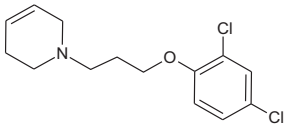	2.6 ± 0.02	66.4 ± 0.2	25.4

[a] $n = 3$.
[b] Selectivity index (S.I.) = IC_{50} of MAO-B/IC_{50} of MAO-A.

typically stronger binding to the enzyme with increasing substrate concentration, the failure to restart the enzyme reaction after complete inhibition by the addition of more substrate can be explained by an uncompetitive inhibition mechanism as indicated by an apparent decrease in both K_m and V_{max} values in the presence of inhibitor and unchanged V_{max}/K_m ratios. The kinetic profile of inhibition by **1** is not consistent with competitive inhibition, although a mixed mechanism has not been ruled out.

The 4-methyl analog **9** and piperidine analog **10** were clearly assigned as reversible inhibitors of MAO-A as established by the observation that increasing substrate concentration blocked the inhibitory effect (Fig. 1B). In addition, analog **9** was found to be a weak inhibitor of MAO-A with a mechanism consistent with mixed noncompetitive inhibition (Fig. 1B, upper panel). With an increase in K_m and decrease in V_{max}, the kinetic mechanism of **9** indicates at least some binding to the catalytic site. A characteristic of the MAO-B selective tetrahydropyridines is an alkyl or aryl group at *C*-4.[30] In the series of compounds **1**–**12**, preference for MAO-A over MAO-B inhibition was apparent. Consistent with the effect of substitution at *C*-4 on MAO selectivity, the 4-methyl tetrahydropyridine **9** was a weak inhibitor of MAO-A in comparison to the activity profile of the 4-unsubstituted analog **1**. Compound **10** represents a hexahydropyridine analog of **1** that displays a simple competitive kinetic mechanism in the inhibition of MAO-A. These results imply that when the tetrahydropyridine moiety was replaced with a 4-methyltetrahydropyridine, or when the double bond was reduced to give a piperidine analog, the binding affinity of inhibitors at putative allosteric sites decrease in comparison with binding to the catalytic site ($K'_i > K_i$ in Scheme 3).

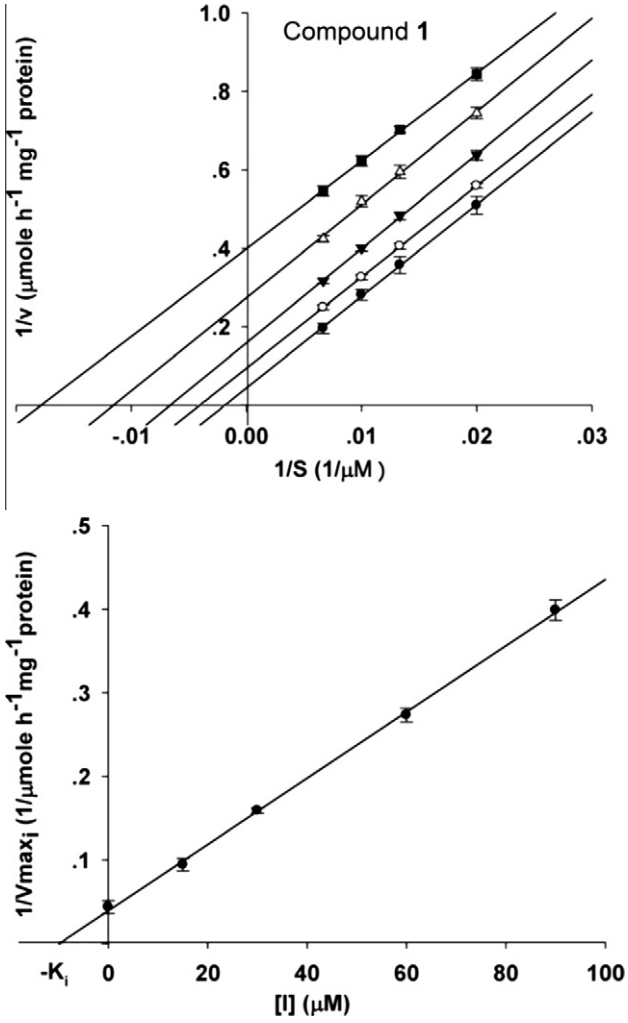

Figure 1A. Representative Lineweaver–Burk plot of the uncompetitive inhibition of recombinant human MAO-A by **1**.Upper panel: MAO-A was incubated(n = 3) with kynuramine (50–150 μM) in the absence (●) or presence of compound **1** at 15 μM (○), 30 μM (▼), 60 μM (△) or 90 μM (■) for 30 min at 37 °C. Lower panel: Replot of data from the Lineweaver–Burk plot, K_i = 9.2 ± 1.9 μM (x-intercept).

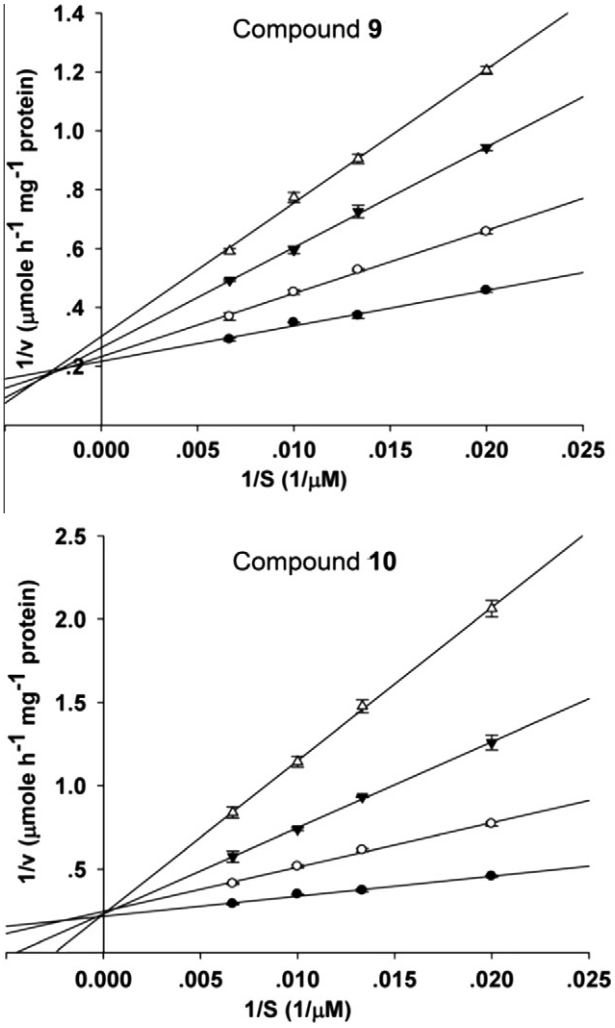

Figure 1B. Representative Lineweaver–Burk plots of the mixed-type inhibition of MAO-A by **9** (Upper panel) and competitive inhibition by **10** (Lower panel). MAO-A was incubated (n = 3)with kynuramine (50–150 μM) in the absence (●) or presence of **9** or **10** at 250 μM (○), 500 μM (▼), or 1000 μM (△)for 30 min at 37 °C.

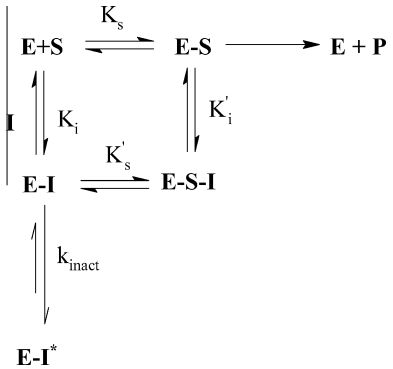

Scheme 3. Proposed kinetic mechanism of inhibition.

The most potent MAO-A inhibitor in the series, clorgyline analog **12**, displayed noncompetitive inhibition of MAO-A (Fig. 1C, upper panel). The K_i value obtained by linear regression of slope replots is consistent with an IC_{50} of a noncompetitive inhibitor.[29] The K_i determined for **12** was 2.2 ± 0.1 μM (Fig. 1C, lower panel). The kinetic mechanism results are consistent with a proposed inhibition mechanism of MAO-A by compound **12** as shown in Eq. 1, where E-I* represents the tightly-bound, slowly-reversible enzyme-inhibitor complex. The presence of both noncompetitive and mechanism-based components may be explained by the contribution from an uncompetitive component associated with the tetrahydropyridine moiety since the inhibitor could bind to either the free enzyme or the enzyme–substrate complex. The kinetic constants and proposed mechanisms are summarized in Table 2.

The time-course of inhibition of kynuramine oxidation by compounds **1**, **9**, **10**, and **12** is illustrated in Figure 2. MPTP is included as a positive control.[31] After an incubation period of 90 min, a second equivalent of substrate was added. Control incubations of kynuramine with MAO-A displayed an increase in product formation over the initial period of 90 min, and a further increase in product formation with additional substrate. In contrast, incubations with kynuramine plus **1** or **12**, inhibited kynuramine metabolism over the first period, and the inhibition was not overcome by adding more substrate at 90 min. Similarly, analogs of **1**, in particular compounds **2**–**8**, did not increase product formation when additional substrate was added (data not shown). Weaker MAO-A inhibitors, **9**, **10**, and MPTP, showed an increase in kynuramine oxidation following addition of substrate at 90 min. At 120 min, fresh enzyme was added to each incubation mixture, and all samples demonstrated an increase in product formation indicating that substrate was still present and the incubation mixture maintained support of MAO-A activity (Fig. 2).

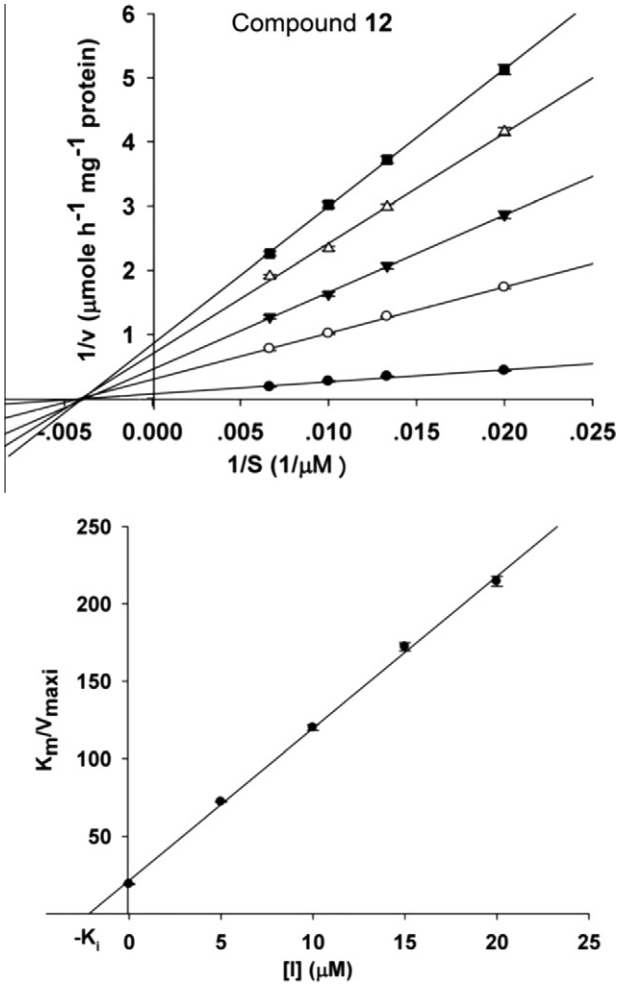

Figure 1C. Upper panel: Representative Lineweaver–Burk plot of the noncompetitive inhibition of MAO-A by **12**. MAO-A was incubated ($n = 3$) with kynuramine (50–150 μM) in the absence (●) or presence of **12** at 5 μM (○), 10 μM (▼),15 μM (△) or 20 μM (■) for 30 min at 37 °C. Lower panel: Replot of data from the Lineweaver–Burk plot, K_i = 2.17 ± 0.09 μM (x-intercept).

2.4. Time-dependent inhibition

Inhibition of MAO-A was time-dependent in the presence of **12** at a concentration of 5 μM. In contrast, tetrahydropyridines**1** and **7** at 50 μM inhibited MAO-A independent of incubation time (Fig. 3). Dependence of inhibition on preincubation time initially indicated that **12** is an irreversible inhibitor of MAO-A. Evaluation of the time-dependence data using a Kitz–Wilson plot[32] indicated that the initial binding of **12** to MAO-A follows pseudo-first order kinetics (Fig. 4, upper panel). Linear regression of the slope replot (Fig. 4, lower panel) gave a straight line that did not pass through zero. From these plots, the estimated inhibitor dissociation constant (K_i) was 7.4 ± 1.3 μM for the initial, reversible interaction between compound **12** and MAO-A. The intercept with the ordinate axis has the value ln $2/k_{inact}$, where k_{inact} is the rate constant for onset of irreversible inhibition. The k_{inact} was estimated to be 0.12 ± 0.01 min^{-1}.

2.5. Reversal of MAO-A inhibition

Figure 5 demonstrates that dialysis completely reversed the inhibition of MAO-A by a high concentration of **1** after 1 h preincubation at 37 °C. Dialysis for 12 h partially reversed MAO-A inhibition by **12**, consistent with reversibility of inhibition. As a positive control, inhibition by clorgyline at 0.5 μM was not reversed by dialysis (Fig. 5). Although the time-dependence studies provided evidence for irreversible inhibition by **12**, the dialysis results are consistent with partially reversible inhibition.

2.6. Covalent intermediate in the inhibition of MAO-A by 12

Trapping experiments in the inhibition of MAO-A with **1** and **12** were done by the addition of the reducing agent, sodium borohydride. With **1** as inhibitor, attempts to trap covalent adducts between inhibitor and enzyme were not successful (Fig. 5). Under the same reducing conditions, treatment with sodium borohydride of MAO-A that had been preincubated with **12** for one hour prior to exposure to substrate shifted the inhibition profile from partially reversible to irreversible (Fig. 5). Control incubations without inhibitor were treated with sodium borohydride to verify that enzyme activity was retained during the experiment.

To address the question of whether inhibition by **12** involves a covalent intermediate, trapping experiments were completed. Stabilization of a covalent reducible intermediate in the reaction of **12** with MAO-A was observed in the presence of the reducing agent, sodium borohydride. Reduction of imine and iminium ion metabolites formed in reactions catalyzed by MAO oxidase with borohydride has been useful in mechanistic studies on cyclopropylamines,[33] serotonin,[34] Ro 41-1049[35] and lazabemide[12] as substrates. Failure to recover MAO-A activity from incubations containing borohydride in comparison to control incubations indicated that a reversible covalent intermediate had been converted

to a covalent structure not readily reversed under dialysis conditions.

2.7. Slowly reversible inhibition

The results from incubations of MAO-A with compound **12** indicate that **12** is a time-dependent, slowly reversible inhibitor of MAO-A in vitro. Irreversible inhibition of MAO is often encountered with substrates containing functional groups that can be bioactivated to electrophilic species. Examples of bioactivated irreversible MAO inhibitors include propargylamines[36,37] and cyclopropylamines.[33] Irreversible MAO inhibitors form covalent adducts with nearby nucleophiles following the oxidative catalytic event. Covalent adducts formed with enzyme protein or with FAD cofactor are considered to be chemically stable and not easily reversed by increasing substrate concentration. Significantly, dialysis is not expected to result in recovery of enzyme activity once the irreversible reaction has taken place. Compound **12** could be described as either an irreversible or reversible MAO-A inhibitor. The time dependency of inhibition of MAO-A by **12** in preliminary experiments supported assignment to the classification of an irreversible inhibitor. Also, excess substrate did not successfully compete with bound inhibitor **12**, which was the same response elicited by the irreversible inhibitor clorgyline. Inconsistent with the behavior of an irreversible inhibitor, inhibition of MAO-A by **12** was partially reversed by dialysis.

An explanation for the MAO-A inhibition behavior of **12** is noncovalent tight-binding of the inhibitor to enzyme.[38] There are several examples of this type of inhibition of monoamine oxidase. Meclobemide and Ro41-1049 show initial competitive inhibition of MAO-A that is followed by time-dependent inhibition.[35] MAO-B that has been inhibited by β-phenylethylamine slowly regains activity upon removal of substrate.[39] MAO-A activity is gradually recovered after repeated washing, sedimentation and resuspension of enzyme following time-dependent inhibition by brofaromine.[40] Inhibition of MAO-B by fluoxetine and norfluoxetine is slowly reversible by dialysis.[41] Inactivation of MAO by allylamine[9] is reversed with benzylamine.[42] Time-dependent inactivation of MAO-B by MPTP is partially reversed by dialysis.[24,43] Generally, tightly-bound or covalently attached enzyme inhibitors that are easily reversed by addition of substrates, other substances, or dialysis are less likely to be categorized as irreversible inhibitors.

A plausible mechanism for the slowly-reversible inhibition of MAO-A involving reversible covalent linkage to the enzyme is proposed in Scheme 4. Analogous to the bioactivation of MPTP by MAO-B,[24] oxidation of tetrahydropyridine **12** catalyzed by MAO-A is proposed to lead to the corresponding dihydropyridinium Michael acceptor **14**. Reversible 1,4-addition of an enzyme nucleophile leads to enamine intermediate **15** that would be reversible to starting enzyme and dihydropyridinium metabolite **14**. Reversible 1,2-addition on **14** by the enzyme nucleophile represents an alternate site of attack. The enamine adduct **15** would also be in equilibrium with the 1,2,3,4-tetrahydropyridinium tautomer **16**. Reduction of iminium ion **16** produces the stable piperidine adduct **17** leading to the observation of irreversible enzyme inhibition. A similar pathway has been proposed by Silverman to explain the inactivation of MAO-B by analogs of MPTP.[44]

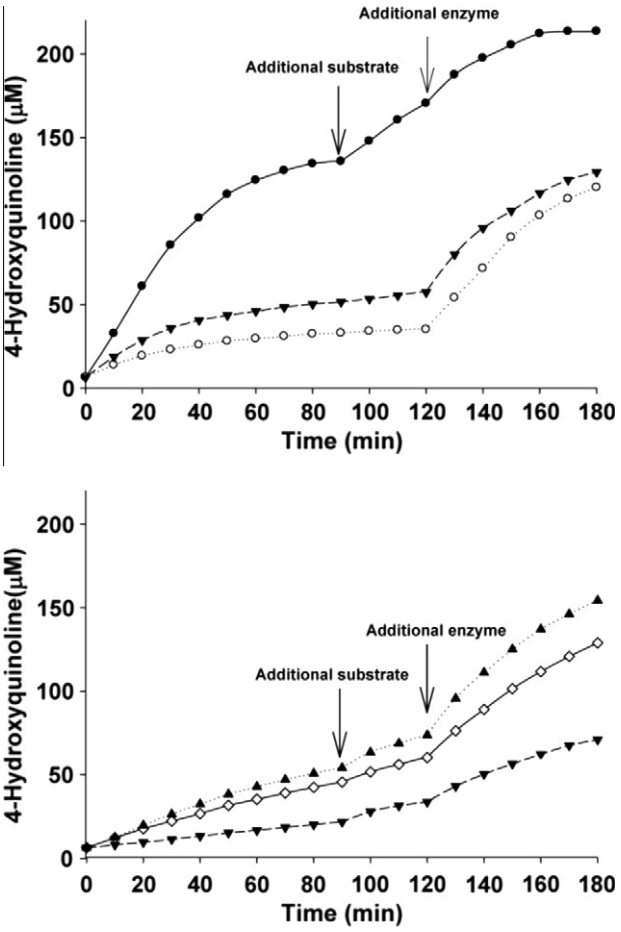

Figure 2. Upper panel: Time course of the formation of the kynuramine metabolite, 4-hydroxyquinoline,by MAO-A in the absence (●) and presence of 1 (○) at 500 μM or 12 (▼) at 5 μM. Lower panel: Time course of the formation of 4-hydroxyquinoline in the presence of 9 (◇) at 6 mM, 10 (▼) at 2 mM, or MPTP (▲) at 50μ M. Additional substrate (150 μM kynuramine) was added at 90 min, and fresh enzyme added at 120 min.

Although the flavin is well-known as the target of irreversible inhibitors of MAO, cysteine residues are candidate allosteric binding site nucleophiles. We hypothesize that a reversible Michael addition reaction between intermediate **14** and one or more of the eight accessible MAO-A cysteines offers a mechanism that is consistent with the noncompetitive or mixed inhibition enzyme kinetics observed, as well as with the result of conversion to irreversible inhibition by borohydride reduction. Proposed intermediate **14**, is expected to be sufficiently stable to allow for diffusion from the hydrophobic active site that do not have cysteine residues near the catalytic site to solvent accessible sites where the cysteine residues are found. Further work is needed to validate this hypothesis. In support of this hypothesis, surface cysteines may be involved in regulating properties of the active site by an allosteric mechanism.[8,16] Furthermore, in the inactivation of MAO-A by cyclopropylamines, C374 is proposed to react by Michael addition

Table 2
Inhibition of MAO A activity in human recombinant mitochondrial fraction

Compound	K_i (μM)	K_i' (μM)	$K_{m\ app}$ (μM)	$V_{m\ app}$ (μm h^{-1} mg^{-1} protein)	Mechanism
1	9.2 ± 1.9	—	217.5 ± 3.6	15.8 ± 2.8	Uncompetitive
9	407.9 ± 5.2	2587 ± 459	56.8 ± 1.5	4.7 ± 0.1	Mixed noncompetitive
10	121.4 ± 4.8	3681 ± 725	60.9 ± 1.5	5.7 ± 0.3	Competitive
12	2.2 ± 0.1	0.90 ± 0.17	209.3 ± 2.3	14.8 ± 0.9	Noncompetitive

$n = 3$

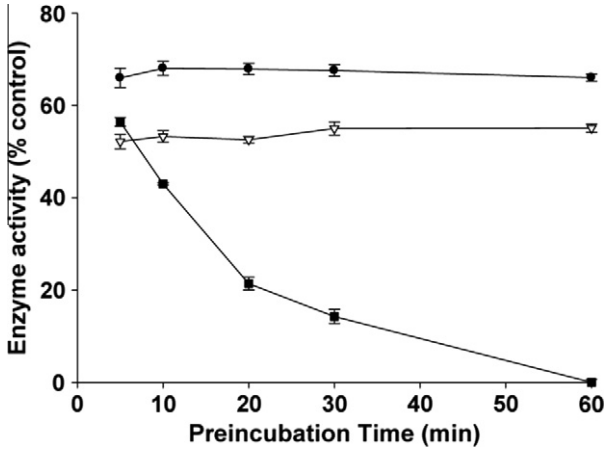

Figure 3. Time-dependent inactivation of MAO-A by 1 (50 μM) (●), 7 (50 μM) (▽) or 12 (5 μM) (■). A plot of the percentage of enzyme activity remaining against preincubation time with MAO-A and inhibitors before addition of kynuramine as substrate. Results are expressed as a percentage of enzyme activity in controls ($n = 3$).

to a corresponding α,β-unsaturated iminium intermediate that had escaped from the hydrophobic active site.[8]

Since the tetrahydropyridines exhibited reversible inhibition, the potential for adverse reactions caused by tyramine potentiation is less than that expected for irreversible inhibitors.[45] Further investigation of the nature of the covalent interaction of 4-unsubstituted tetrahydropyridines will be needed to clarify the mechanism of reversible inactivation of MAO-A.

2.8. Neurotoxicity assessment

The tetrahydropyridine compounds studied are structurally similar to the tetrahydropyridine neurotoxin, MPTP. 4-Substituted 1,2,3,6-tetrahydropyridines, such as MPTP, are well-described inhibitors and substrates of MAO.[20,42,46] Neurotoxicity of MPTP and related 4-substituted tetrahydropyridines is closely associated with mechanism-based activation by MAO-B.[24,31,39] Selective MAO-A inhibitors are less likely than MAO-B inhibitors to exhibit neurotoxicity.[30] In the present series, MAO inhibition by **1** was not associated with MPTP-like neurotoxicity. Compound **1** did not reduce striatal tyrosine hydroxylase, increase striatal GFAP, or affect dopamine and serotonin concentrations, which is consistent with a lack of dopaminergic and serotonergic neurotoxicity. MPTP administered as a positive control resulted in the expected decrement in tyrosine hydroxylase and increase in striatal GFAP at 72 hours post dosing, which is a finding consistent with damage to dopaminergic nerve terminals. Further indication that **1** did not disrupt dopamine function was found in measurements of brain levels of dopamine metabolite concentrations following treatment (data not shown). Also, **1** did not affect brain concentrations of dopamine or its metabolites, providing further evidence that dopamine function was not altered.

3. Conclusions

Within a small series of N-substituted tetrahydropyridines, several kinetic mechanisms of inhibition of MAO-A were observed ranging from mixed mechanisms to mechanism-dependent inhibition involving a reversible covalent intermediate. In a broader sense, tetrahydropyridine analogs may serve as useful probes for further investigation of binding characteristics of MAO. The most potent inhibitor in the series, tetrahydropyridine **12**, can be considered as a lead structure of a potentially new class of MAO-A

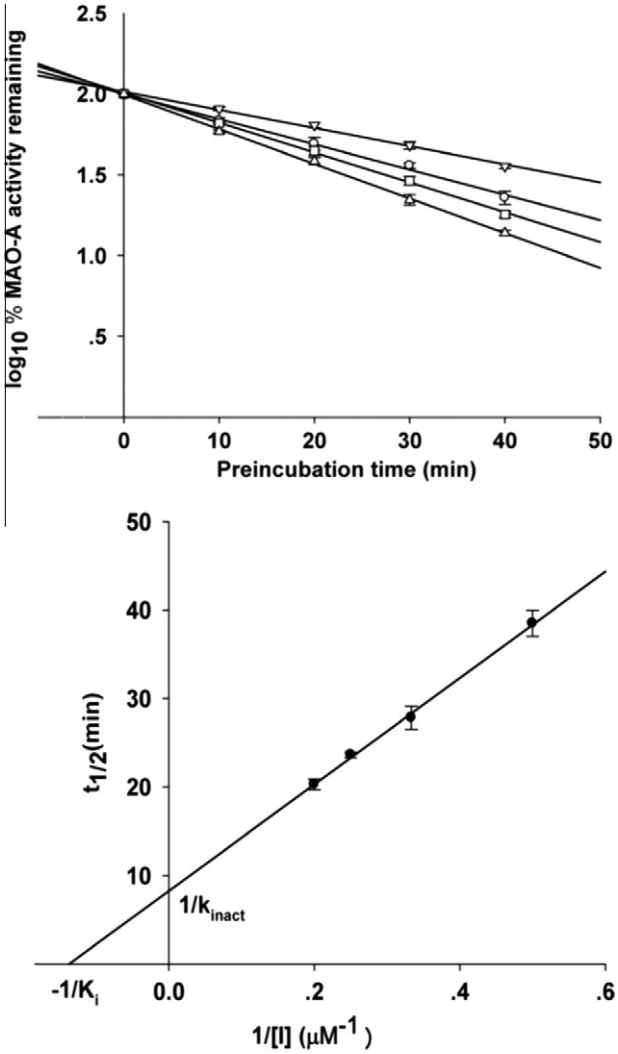

Figure 4. Upper panel: Effect of **12** concentration on the rate of onset of MAO-A inhibition. MAO-A was preincubated with **12** at 2 μM (▽), 3 μM (○), 4 μM (□), 5 μM (△) before adding substrate kynuramine (150 μM). Results are expressed as a percentage of activity of controls, means ± SD from three experiments. Lower panel: Slope replot of the data. The reciprocal of the x-intercept provides a K_i of 7.4 ± 1.3 μM and the reciprocal of y-intercept represents a k_{inact} of 0.12 ± 0.01 min^{-1}.

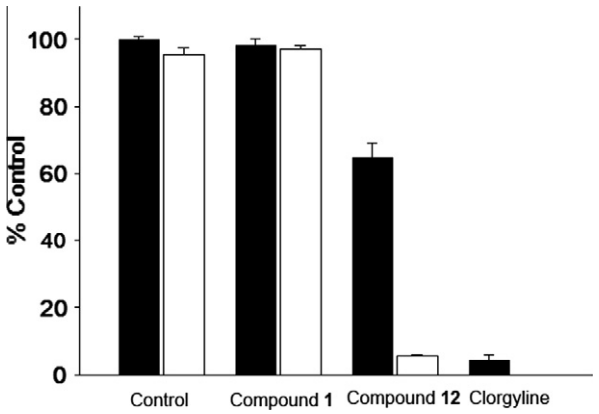

Figure 5. Effect of dialysis on the inhibition of MAO-A by **1**and **12** in the absence (■) or presence of NaBH4 (□).Clorgyline was a positive control for irreversible inhibition. Results are expressed as a percentage of enzyme activity in controls ($n = 3$).

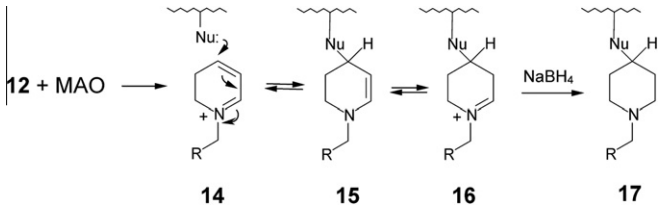

Scheme 4. Potential mechanism for the interaction of **12** with MAO-A.

selective inhibitors characterized by reversible covalent inhibition that is unlikely to be associated with tyramine potentiation.

4. Experimental section

All chemical reagents for synthesis were supplied by Sigma–Aldrich (St. Louis, MO) and used without further purification. Basic alumina was purchased from Sorbent Technologies (Atlanta, GA). Reaction progress was monitored by thin layer chromatography on pre-coated plastic plates (silica gel 60 F254, 0.25 mm thickness) purchased from Macherey–Nagel Company (Easton, PA). Melting points were determined on a Thomas Hoover capillary melting point apparatus. ^{1}H NMR spectra obtained in deuterated chloroform ($CDCl_3$) were recorded at 300 MHz. Chemical shifts are reported as δ values in parts per million (ppm) relative to the residual solvent peak and coupling constants are reported as *J* values in Hertz. High resolution electrospray ionization mass spectra (HRMS) were recorded on a Finnigan FT mass spectrometer.

4.1. *N*-Phenylalkyl substituted 1,2,3,6-tetrahydropyridine derivatives (1–9)

Pyridine or 4-picoline (1 mmol) and phenylalkyl halide derivatives (1.2 mmol) were condensed at 140 °C to yield the corresponding *N*-phenylalkyl pyridinium halides.[26,47] The products were solidified from diethyl ether. Sodium borohydride (5 mmol) was added in portions to a stirred solution of the *N*-phenylalkyl pyridinium halide (1 mmol) in 30 mL of dry methanol at 0 °C. The mixture was stirred for an additional 4 h, and the solvent was subsequently removed under reduced pressure. The residue in 30 mL of water was extracted with ethyl acetate (3 × 20 mL). The combined organic layers were dried ($MgSO_4$), filtered, and concentrated to near dryness under reduced pressure. The crude tetrahydropyridine was purified by column chromatography on silica using 1% triethylamine in hexane/ethyl acetate (1:5). The obtained product was eluted through a basic alumina column with CH_2Cl_2 to yield the corresponding *N*-phenylalkyl substituted 1,2,3,6-tetrahydro-pyridine, which was converted to the hydrochloride salt by dissolving the free base in 10 mL of 120 mM ethanolic HCl and evaporating to afford pure tetrahydropyridine hydrochloride.

4.2. 1-(2-Phenylethyl)-1,2,3,6-tetrahydropyridine (1)

Compound **1** was prepared using the procedure as described above in 80.1% yield as a colorless solid. ^{1}H-NMR ($CDCl_3$) (free base): δ (ppm) = 7.4–7.2 (m, 5H, ArH); 5.9–5.8 (m, 1H, vinylic H); 5.8–5.7 (m, 1H, vinylic H); 3.2–3.1 (d, 2H, C-6 H); 2.9–2.8 (m, 2H, N-CH_2); 2.8–2.6 (m, 4H, C-2 H and CH_2Ar); 2.3–2.2 (m, 2H, C-3 H). HRMS-ESI $[M+H]^+$ calcd for $C_{13}H_{17}N$, 188.1434; found, 188.1434; mp of **1·HCl**, 208–209 °C; lit. [48] mp 195–197 °C.

4.3. 1-[2-(4-Fluorophenyl)ethyl]-1,2,3,6-tetrahydropyridine (2)

Compound **2** was prepared using the procedure as described above in 89.4% yield as a colorless solid. ^{1}H-NMR ($CDCl_3$) (free base): δ (ppm) = 7.2 (d, 2H, *J* = 8.6 Hz, ArH); 7.0 (d, 2H, *J* = 8.6 Hz, ArH); 5.8 (m, 1H, vinylic H); 5.7 (m, 1H, vinylic H); 3.1–3.0 (d, 2H, C-6 H); 2.9–2.8 (m, 2H, N-CH_2); 2.8–2.6 (m, 4H, C-2 H and CH_2Ar); 2.3–2.2 (m, 2H, C-3 H). HRMS-ESI $[M+H]^+$ calcd for $C_{13}H_{16}FN$, 206.1340; found, 206.1340; mp of **2·HCl**, 192–193 °C.

4.4. 1-[2-(4-Methoxyphenyl)ethyl]-1,2,3,6-tetrahydropyridine (3)

Compound **3** was prepared using the procedure as described above in 78.8% yield as an off-white solid. ^{1}H-NMR ($CDCl_3$) (free base): δ (ppm) = 7.2 (d, 2H, *J* = 8.7 Hz, ArH); 6.9 (d, 2H, *J* = 8.7 Hz, ArH); 5.8 (m, 1H, vinylic H); 5.7 (m, 1H, vinylic H); 3.8 (s, 3H, 4-methoxy H); 3.1 (m, 2H, C-6 H); 2.9–2.8 (m, 2H, N-CH_2); 2.7–2.6 (m, 4H, C-2 H and CH_2Ar); 2.3–2.2 (m, 2H, C-3 H). HRMS-ESI $[M+H]^+$ calcd for $C_{14}H_{19}NO$, 218.1539; found, 218.1540; mp of **3·HCl**, 198–200 °C.

4.5. 1-[2-(3,4-Methoxyphenylethyl]-1,2,3,6-tetrahydro-pyridine (4)

Compound **4** was prepared using the procedure as described above in 75.7% yield as an off-white solid**.** ^{1}H-NMR ($CDCl_3$) (free base): δ (ppm) = 6.8–6.7 (m, 3H, ArH); 5.8 (m, 1H, vinylic H); 5.7 (m, 1H, vinylic H); 3.9 (s, 3H, methoxy H); 3.85 (s, 3H, methyoxy H); 3.1 (m, 2H, C-6 H); 2.9–2.8 (m, 2H, N-CH_2); 2.7–2.6 (m, 4H, C-2 H and CH_2Ar); 2.3–2.2 (m, 2H, C-3 H). HRMS-ESI $[M+H]^+$ calcd for $C_{15}H_{21}NO_2$, 248.1645; found, 248.1645; mp of **4·HCl**, 208–209 °C.

4.6. 1-(3-Phenylpropyl)-1,2,3,6-tetrahydropyridine (5)

Compound **5** was prepared using the procedure as described above in 70.4% yield as a colorless solid. ^{1}H-NMR ($CDCl_3$) (free base): δ (ppm) = 7.4–7.2 (m, 5H, ArH); 5.8 (m, 1H, vinylic H); 5.7 (m, 1H, vinylic H); 3.1–3.0 (m, 2H, C-6 H); 2.8–2.7 (t, 2H, *J* = 6.3 Hz, N-CH_2); 2.7–2.6 (t, 2H, *J* = 6.5 Hz, C-2 H); 2.6–2.5 (t, 2H, *J* = 6.3 Hz, CH_2Ar); 2.3–2.2 (m, 2H, C-3 H); 2.0–1.9 (m, 2H, alkyl CH_2). HRMS-ESI $[M+H]^+$ calcd for $C_{14}H_{19}N$, 202.1590; found, 202.1590; mp of **5·HCl**, 158–160 °C.

4.7. 1-[2-(2,4-Dichlorophenyl)ethyl]-1,2,3,6-tetrahydro-pyridine (6)

Compound **6** was prepared using the procedure as described above in 78.5% yield as a colorless solid. ^{1}H-NMR ($CDCl_3$) (free base): δ (ppm) = 7.5–7.4 (d, 1H, *J* = 2.5 Hz, ArH); 7.3–7.2 (m, 2H, ArH); 5.9–5.8 (m, 1H, vinylic H); 5.7–5.8 (m, 1H, vinylic H); 3.2 (m, 2H, C-6 H); 3.1–3.0 (m, 2H, N-CH_2); 2.8–2.7 (m, 4H, C-2 H and CH_2Ar); 2.4–2.3 (m, 2H, C-3 H) (yield =78.5%). HRMS-ESI $[M+H]^+$ calcd for $C_{13}H_{15}Cl_2N$, 256.0654; found, 256.0654; mp of **6·HCl**, 204–205 °C.

4.8. 1-[2-(4-Nitrophenyl)ethyl]-1,2,3,6-tetrahydropyridine (7)

Compound **7** was prepared using the procedure as described above in 86.5% yield as a pale yellow solid. ^{1}H-NMR ($CDCl_3$) (free base): δ (ppm) = 8.2 (d, 2H, *J* = 8.5 Hz, ArH); 7.4 (d, 2H, *J* = 8.5 Hz, ArH); 5.8 (m, 1H, vinylic H); 5.7 (m, 1H, vinylic H); 3.1 (m, 2H, C-6 H); 3.0–2.9 (m, 2H, N-CH_2); 2.8–2.6 (m, 4H, C-2 H and CH_2Ar); 2.3–2.2 (m, 2H, C-3 H). HRMS-ESI $[M+H]^+$ calcd for $C_{13}H_{16}N_2O_2$, 233.1285; found, 233.1285; mp of **7·HCl**, 202–204 °C.

4.9. 1-Phenylmethyl-1,2,3,6-tetrahydropyridine (8)

Compound **8** was prepared using the procedure as described above in 87.7% yield as an off-white solid. ^{1}H-NMR ($CDCl_3$) (free base): δ (ppm) = 7.4–7.2 (m, 5H, ArH); 5.8 (m, 1H, vinylic H), 5.7 (m, 1H, vinylic H); 3.6 (s, 2H, benzylic H); 3.1–3.0 (m, 2H, J = 6.5 Hz, C-6 H); 2.6 (t, C-2 H); 2.2 (m, 2H, C-3 H). HRMS-ESI $[M+H]^+$ calcd for $C_{12}H_{15}N$, 174.1277; found, 174.1277; mp of **8·HCl**, 200–203 °C; lit. [49] mp 195–197 °C.

4.10. 1-(2-Phenylethyl)-4-methyl-1,2,3,6-tetrahydropyridine (9)

Compound **9** was prepared using the procedure as described above in 80.5% yield as a colorless solid; ^{1}H-NMR ($CDCl_3$) (free base): δ (ppm) = 7.4–7.2 (m, 5H, ArH); 5.5–5.4 (m, 1H, vinylic H); 3.1 (m, 2H, C-6 H); 3.0–2.9 (m, 2H, N-CH_2); 2.8–2.7 (m, 4H, C-2 H and CH_2Ar); 2.2–2.1 (m, 2H, C-3 H); 1.7 (s, 3H, 4-methyl H); lit. [50] 1.7 (s, 3H, 4-methyl H). HRMS-ESI $[M+H]^+$ calcd for $C_{14}H_{19}N$, 202.1590; found, 202.1590; mp of **9·HCl**, 223–225 °C, lit. [50] mp 226 °C.

4.11. 1-(2-Phenylethyl)piperidine hydrochloride (10·HCl)

Phenylacetaldehyde (90%) (0.78 g, 5.87 mmol) and piperidine (0.50 g, 5.87 mmol) were vigorously stirred in 30 mL methanol at 0 °C. The solution mixture was acidified (pH 4–5) with 99% formic acid. Sodium borohydride (0.67 g, 17.6 mmol) was added in portions with stirring to the mixture and stirred for an additional 4 h. The solvent was subsequently removed under reduced pressure. The residue in 30 mL of water was extracted with ethyl acetate (3 × 30 mL). The combined organic layers were dried ($MgSO_4$), filtered, and concentrated to near dryness under reduced pressure. The crude piperidine was purified by column chromatography on silica column using 1% triethylamine in hexane/ethyl acetate (1:5). The obtained product was eluted through a basic alumina column eluted with CH_2Cl_2 to yield 1-(2-phenylethyl) piperidine (**10**), which was converted to the hydrochloride salt by dissolving the free base in 10 mL of ethanolic HCl (7.5 mmol) and evaporating to afford pure hydrochloride salt in 72.1% yield as a colorless solid. ^{1}H-NMR ($CDCl_3$) (free base): δ (ppm) = 7.4–7.2 (m, 5H, ArH); 2.9–2.8 (m, 2H, N-CH_2); 2.6–2.5 (m, 2H, CH_2Ar); 2.5–2.4 (m, 4H, C-2 H and C-6 H); 1.7–1.6 (m, 4H, C-3 H and C-5 H); 1.5–1.4 (m, 2H, C-4 H), lit. [51] 1.45 (m, 2 H, ring γ-CH_2). HRMS-ESI $[M+H]^+$ calcd for $C_{13}H_{19}N$, 190.1590; found, 190.1590; mp of **10·HCl**, 220–222 °C.

4.12. 1-[3-(2,4-Dichlorophenoxy)propyl]-1,2,3,6-tetrahydropyridine (12)

A round-bottomed flask was charged with 2,4-dichlorophenol (1.0 g, 6.13 mmol) dissolved in 2 mL of dry dimethylacetamide. NaH (0.22 g, 9.20 mmol) was added and the solution was stirred under nitrogen atmosphere at 30 °C for 30 min. The reaction mixture was added dropwise over 30 min to rapidly stirred 1,3-dibromopropane (3.72 g, 18.4 mmol) and the reaction was heated to 70 °C for an additional 4 h. The reaction was monitored by TLC and the product appeared with an R_f = 0.6 (3:1 hexane/ethyl acetate). The reaction mixture was subsequently quenched with water (10 mL) and the product was extracted with ether (2 × 30 mL). The combined organic layers were dried ($MgSO_4$), filtered, and concentrated to near dryness under reduced pressure. The crude residue was purified by column chromatography on silica column using hexane/ethyl acetate (4:1) to provide 1-(3-Bromopropoxy)-2,4-dichlorobenzene (**11**) in 69.8% yield as a colorless oil. ^{1}H-NMR ($CDCl_3$): δ (ppm) = 7.4 (d, 1H, J = 2.7 Hz, ArH); 7.2 (dd, 1H, J = 2.7, 8.7 Hz, ArH); 6.9 (d, 1H, J = 8.7 Hz, ArH); 4.2–4.1 (t, 2H, J = 6.3 Hz, O-CH_2); 3.7–3.6 (t, 2H, J = 6.3 Hz, Br-CH_2); 2.4–2.3 (m, 2H, J = 6.3 Hz, CH_2).Without further purification, *N*-alkylation of pyridine (0.28 g, 3.52 mmol) with **11** (1.0 g, 3.52 mmol) was carried out at 140 °C for 4 h. The crude product was recrystallized from diethyl ether to yield 1-(3-(2,4-dichlorophenoxy) propyl) pyridinium bromide (1.06 g, 83.1%). Without further purification, reduction of the intermediate with $NaBH_4$ (5.5 g, 14.6 mmol) in methanol was conducted at 0 °C for 4 h. The crude tetrahydropyridine was purified by column chromatography on silica column using 1% triethylamine in hexane/ethyl acetate (1:5). The obtained product was eluted through a basic alumina column by using CH_2Cl_2 to yield **12**, which was converted to the hydrochloride salt by dissolving the free base in 10 mL of ethanolic HCl (1.2 mmol) and evaporating to afford pure **12·HCl** in 67.3% yield as a colorless solid. ^{1}H-NMR ($CDCl_3$) (free base): δ (ppm) = 7.4 (d, 1H, J = 2.7 Hz, ArH); 7.2 (dd, 1H, J = 2.7, 8.9 Hz, ArH); 6.9 (d, 1H, J = 8.9 Hz, ArH); 5.8–5.7 (m, 1H, vinylic H); 5.7–5.6 (m, 1H, vinylic H); 4.1 (t, 2H, J = 6.3 Hz, O-CH_2); 3.1 (m, 2H, C-6 H); 2.8–2.6 (m, 4H, C-2 H and N-CH_2); 2.3–2.2 (m, 2H, C-3 H); 2.2–2.0 (m, 2H, J = 6.3 Hz, CH_2). HRMS-ESI $[M+H]^+$ calcd for $C_{14}H_{17}Cl_2NO$, 286.0760; found, 286.0760; mp of **12·HCl**, 136–137 °C.

4.13. Biology

Kynuramine dihydrobromide, benzyl amine, benzaldehyde and 4-hydroxyquinoline were supplied by Sigma–Aldrich (St. Louis, MO) at the highest purity available (>99%). MAO-A and MAO-B (5 mg/mL), obtained from insect cells containing recombinant human enzyme, were supplied by Sigma–Aldrich (St. Louis, MO), prealiquoted and stored at −80 °C. All enzymatic reactions with MAO-A (0.005 mg/mL) or MAO-B (0.01 mg/mL) were carried out in 0.1 M sodium phosphate buffer pH 7.4, made isotonic with NaCl (PBS). All UV-vis spectral studies of MAO-A were carried out on a Beckman-DU640 spectrophotometer. The chromatographic system consisted of a binary pump (LC-10 ADvp), a solvent degasser (DGU-14 A), an autosampler (SIL-10 ADvp), an oven (CTO-10ASvp) and UV-vis detector (SPD-10Avp), all from Shimadzu. A Zorbax 5 μ phenyl analytical column (150 × 4.6 mm, 5 μm) (Agilent) was used for measuring MAO-B inhibition.

4.14. MAO-A Inhibition assay

The enzymatic reaction was carried out in sodium phosphate buffer (0.1 M, pH 7.4, made isotonic with NaCl) (0.1 M PBS) containing MAO-A (0.005 mg/mL), various concentrations of the tetrahydropyridine analogs (0–7000 μM) and kynuramine dihydrobromide (150 μM). The final volume of the reaction was 500 μL. Stock solutions of the tetrahydropyridine analogs (compound **1**–**10**, **12**) were prepared in 0.1 M PBS. The reactions were incubated for 60 min at 37 °C. The concentrations of remaining kynuramine in the reactions were determined by measuring the UV intensity at a wavelength of 360 nm.[43] Quantitative estimations of kynuramine were made by means of linear calibration curves ranging from 30 to 300 μM. Each calibration standard was prepared to a final volume of 1 mL in 0.1 M PBS. The activity of enzyme was expressed as the change in absorbency over time. IC_{50} values were determined by plotting the percentage of remaining enzyme activities versus the logarithm of the inhibitor concentration to obtain a sigmoidal dose–response curve. IC_{50} values were determined in triplicate and were expressed as means ± standard deviation (SD) by using SigmaPlot software (Systat Software Inc.).

4.15. MAO-B Inhibition assay

The enzymatic reaction was carried out in 0.1 M PBS containing MAO-B (0.01 mg/mL), various concentrations of the tetrahydropyridine analogs (0–7000 μM) and benzylamine

hydrochloride. The final concentration of benzylamine in the reactions was 1000 μM. For the determination of enzyme activity, the enzyme incubation mixture contained the following component in a total volume of 500 μL, 350 μL of 0.1 M PBS, 100 μL of enzyme, and 50 μL of benzylamine hydrochloride. Stock solutions of the tetrahydropyridine analogs (compounds **1**–**10**, **12**) were prepared in 0.1 M PBS. The reactions were incubated for 30 min at 37 °C and terminated with the addition of 50 μL of 1 M perchloric acid prior to centrifugation for 20 min at 13,500*g*. The concentrations of benzaldehyde product formed were determined by an HPLC method.[52] Elutions were done isocratically using mobile phase containing 30% acetonitrile in water at a flow rate of 1.0 mL/min. Eluted components were detected by ultraviolet absorption (UV) of 254 nm. The column oven temperature was 33 °C. Quantitative estimations of benzaldehyde were estimated from a linear calibration curve ranging from 1 to 100 μM. Each calibration standard was prepared to a final volume of 1 mL in 0.1 M PBS. IC_{50} values were determined by plotting the percentage of remaining enzyme activities versus the logarithm of the inhibitor concentration to obtain a sigmoidal dose–response curve. IC_{50} values were determined in triplicate and were expressed as means ± standard deviation (SD) by using SigmaPlot software (Systat Software Inc.). Selectivity of MAO-A versus MAO-B was calculated as a Selectivity Index (SI) from a ratio of MAO-B IC_{50} value divided by the MAO-A IC_{50} value.

4.16. MAO-A enzyme kinetics

The initial rates of oxidation at four concentrations of kynuramine in the absence and presence of four concentrations of the inhibitors (compounds **1**, **9**, **10** and **12**) were determined. Where recombinant human MAO-A was used as enzyme source, compounds **1**, **9**, **10** and **12** at concentrations of 15–90 μM, 250–1000 μM, 250–1000 μM and 5–20 μM, respectively, were evaluated as inhibitors and kynuramine (50–150 μM) served as substrate. All enzymatic reactions were performed in 0.1 M PBS at 37 °C. The final volume of the reactions was 500 μL. Quantitative estimations of kynuramine were made by means of a linear calibration curve ranging from 30 to 300 μM. Each calibration standard was prepared to a final volume of 1 mL in 0.1 M PBS. Determinations were performed in triplicate and statistical data refer to the number of replicate experiments in each case. Linear regression analysis was performed using SigmaPlot software (Systat Software Inc.).

4.17. Time-dependent MAO-A inhibition studies and Kitz-Wilson plots

In studies of the dependence of inhibition on concentration and incubation time of compound **1** and its analogs for MAO-A, compounds **1**, **7** and **12** were evaluated at 50 μM, 50 μM and 5 μM, respectively at 37 °C in 0.1 M PBS for 5–90 min. Samples were then diluted 50-fold in buffer containing the substrate to start the enzyme reaction. Control incubations were used in which the inhibitor solution was replaced by an equivalent volume of 0.1 M PBS. The kinetics of the interaction between compound **12** and MAO-A were further examined by the method of Kitz and Wilson.[32] MAO-A was preincubated at 37 °C with a range of concentrations of compound **12** (2–5 μM) or 0.1 M PBS (control) for 0, 10, 20, 30 or 40 min prior to kynuramine addition. The final volume of the reactions was 500 μL. Following the disappearance of kynuramine, samples were incubated for 30 min and enzyme activities determined as described above. Results represent the means ± standard deviation (n = 3). Linear regression analysis was performed using SigmaPlot software (Systat Software Inc.).

4.18. Reversal of inhibition of MAO-A by dialysis

Dialysis was performed on MAO-A samples that were preincubated at 37 °C for 1 h in the absence of kynuramine substrate with compounds **1** (500 μM), **12** (5 μM) and clorgyline (0.5 μM) prepared to the final volume of 1 mL in 0.1 M PBS. Aliquots (500 μL) of each incubation mixture were pipetted into dialysis tubing (size 3; diameter, 11.5 mm; MWCO 3,500; Spectra/Por molecular porous membranes) (Spectrum Laboratories, Inc., Rancho Dominguez, CA) and then were dialyzed at 0 °C against 250 mL of 0.1 M PBS overnight. MAO-A activity in the dialysates was determined by measuring product formation at 310 nm using 150 μM kynuramine as substrate over 60-min incubations at 37 °C. Quantitative estimations of 4-hydroxyquinoline were made using a linear calibration curve ranging from 20 to 150 μM. Each calibration standard was prepared to a final volume of 1 mL in 0.1 M PBS. Results represent means ± standard deviation (SD) (n = 3).

4.19. Reduction of enzyme complex with sodium borohydride

After preincubation of MAO-A for 60 min with compounds **1** (500 μM), **12** (5 μM) and clorgyline (0.5 μM), 5 μL of 300 mM $NaBH_4$ in water was added and the mixture cooled in a water bath at 0 °C for 15 min. The resulting mixture was dialyzed and residual MAO-A activity measured as above.

4.20. Animals

Female C57BL/6 J mice, 3–4 months of age were purchased from the Jackson Laboratories (Bar Harbor, ME). The colony room was controlled for temperature (22 ± 2 °C) and humidity (30–40%) and was maintained on a 12-h light/12-h dark cycle. Mice were fed Teklad 7913 irradiated chow (Harlan Teklad, Indianapolis, IN); access to chow and water was allowed ad libitum. The animal protocol governing the experiments was approved by the Institutional Animal Care and Use Committee of the Centers for Disease Control and Prevention-National Institute for Occupational Safety and Health. The Animal Care and Use Facility is accredited by the American Association for Accreditation of Laboratory Animal Care.

4.21. Toxicant administration and brain tissue preparation

Mice were administered a single dose of **1** (25 mg/kg, sc). In addition, MPTP (12.5 mg/kg, sc) was used as a positive control; 0.9% saline served as a vehicle control for all compounds. Mice were sacrificed 72 h after administration of each compound. This time point yields maximum increases in GFAP and maximum decreases in TH after MPTP administration, indices that reflect induction of astrogliosis and loss of dopaminergic nerve terminals, respectively, due to dopaminergic neurotoxicity. After sacrifice, brains were removed and the striatum was dissected, free-hand, using small forceps and the aid of a magnifying lens. The selected regions from one side of the brain were frozen for subsequent analysis of brain amines and the regions from the other side of the brain were homogenized in hot (80–90 °C) 1% (w/v) SDS for subsequent analysis by specific ELISA.

4.22. GFAP and TH ELISA

Glial fibrillary acidic protein (GFAP) and tyrosine hydroxylase (TH) were assayed using the detergent-based sandwich enzyme-linked immunosorbent assays (ELISAs). Detailed protocols for the GFAP ELISA procedure have been described.[52–55] The modifications used for assaying TH also have appeared.[56] Briefly, 'capture' antibodies were coated on the wells of Immunlon-2 microtiter plates (Thermo Labsystems, Franklin, MA). The SDS homogenates of

specific brain regions and standards were diluted in PBS containing 0.5% Triton X-100. Nonspecific binding was blocked with 5% nonfat dry milk in PBS and then aliquots of the homogenates and standards were added to the wells and incubated. Following four sequential washes, a different host specifies antibody to GFAP or TH from the ones used as 'capture' were added to 'sandwich' the antigen between the antibodies. An alkaline phosphatase or peroxidase conjugated secondary with fluorogenic substrate was used as a reporter for quantification of GFAP and TH, respectively, via spectrophotometry and fluorometry.

4.23. Measurement of catecholamines and catecholamine metabolites

Dopamine, serotonin and their metabolites were quantified by high performance liquid chromatography with electrochemical detection (HPLC_EC; Waters). Striata were homogenized in 300 μL of ice-cold 0.2 M perchloric acid, containing 1 μM dihydroxybenzylamine as internal standard, and centrifuged at 10,000*g* for 10 min at 4 °C. The supernatant was filtered through a 0.2 μm membrane, and 10 μL was injected from a temperature-controlled (4 °C) automatic sample injector (Waters 717 plus Autosampler) connected to a Waters 515 HPLC pump. Analytes were separated on a C18 reverse-phase column (LC-18RP; Waters SYMMETRY, 25 cm × 4.6 mm; 5 μm), electrochemically detected (Waters 464 Pulsed Electrochemical Detector; range 10 nA, potential +0.7 V), and analyzed using Millennium software (Waters). The mobile phase, pH 3.0, for isocratic separation consisted of dibasic sodium phosphate (75 mM), octane sulfonic acid (1.7 mM), acetonitrile (10% v/v), and EDTA (25 μM). Flow rate was maintained at 1 mL/min, dopamine, 3,4-dihydroxyphenylacetic acid (DOPAC), homovanillic acid (HVA), serotonin, and 5-hydroxyindoleacetic acid (5-HIAA) standards (0.5–25 pmol) were prepared in 0.2 M perchloric acid containing dihydroxybenzylamine. Recovery of each analyte was adjusted with respect to the internal standard and quantified from a standard curve. The levels of dopamine, serotonin and their metabolites were expressed as micrograms per gram of wet tissue.

Acknowledgments

Financial support was provided by the Thailand Research Fund through the Royal Golden Jubilee Ph.D Program (Grant No. PHD/0217/2548) to W. Wichitnithad and U. Nimmannit. Technical assistance from James D. Thornton and Rachel Brown is appreciated. Support from the mass spectrometry laboratory at West Virginia University is acknowledged.

Supplementary data

Supplementary data associated with this article can be found, in the online version, at doi:10.1016/j.bmc.2011.10.038. These data include MOL files and InChiKeys of the most important compounds described in this article.

References and notes

1. Bolasco, A.; Carradori, S.; Fioravanti, R. *Expert Opin. Ther. Patents* **2010**, *20*, 909.
2. Youdim, M. B. H.; Edmondson, D.; Tipton, K. F. *Nat. Rev. Neurosci.* **2006**, *7*, 295.
3. Stahl, S. M.; Felker, A. *CNS Spectr.* **2008**, *10*, 855.
4. Edmondson, D. E.; Binda, C.; Mattevi, A. *Arch. Biochem. Biophys.* **2007**, *464*, 269.
5. De Colibus, L.; Li, M.; Binda, C.; Lustig, A.; Edmondson, D. E.; Mattevi, A. *Proc. Natl. Acad. Sci. U.S.A.* **2005**, *102*, 12684.
6. Binda, C.; Newton-Vinson, P.; Hubálek, F.; Edmondson, D. E.; Mattevi, A. *Nat. Struct. Biol.* **2002**, *9*, 22.
7. Binda, C.; Hubálek, F.; Li, M.; Herzig, Y.; Sterling, J.; Edmondson, D. E.; Mattevi, A. *J. Med. Chem.* **2005**, *48*, 8148.
8. Vintém, A. P.; Price, N. T.; Silverman, R. B.; Ramsay, R. R. *Bioorg. Med. Chem.* **2005**, *13*, 3487.
9. Rando, R. R.; Eigner, A. *Mol. Pharmacol.* **1977**, *13*, 1005.
10. Binda, C.; Li, M.; Hubalek, F.; Restelli, N.; Edmondson, D. E.; Mattevi, A. *Proc. Natl. Acad. Sci. U.S.A.* **2003**, *100*, 9750.
11. Paech, C.; Salach, J. I.; Singer, T. P. *J. Biol. Chem.* **1980**, *255*, 2700.
12. Cesura, A. M.; Gottowik, J.; Lahm, H. W.; Lang, G.; Imhof, R.; Malherbe, P.; Röthlisberger, U.; Da Prada, M. *Eur. J. Biochem.* **1996**, *236*, 996.
13. Fu, R. C.; Liu, X.-F.; Chen, S. *J. Neurochem.* **1990**, *55*, 813.
14. Weyler, W.; Salach, J. I. *J. Biol. Chem.* **1985**, *260*, 13199.
15. Wu, H. F.; Chen, K.; Shih, J. C. *Mol. Pharmacol.* **1993**, *43*, 888.
16. Ramsay, R. R.; Jones, T. Z.; Hynson, R. M. *Med. Sci. Monit.* **2005**, *11*, SR15.
17. McDonald, G. R.; Olivieri, A.; Ramsay, R. R.; Holt, A. *Pharmacol Res.* **2010**, *62*, 475.
18. Jones, T. Z.; Giurato, L.; Guccione, S.; Ramsay, R. R. *FEBS J.* **2007**, *274*, 1567.
19. Bonivento, D.; Milczek, E. M.; McDonald, G. R.; Binda, C.; Holt, A.; Edmondson, D. E.; Mattevi, A. *J. Biol. Chem.* **2010**, *285*, 36849.
20. Mabic, S.; Castagnoli, N. *J. Med. Chem.* **1996**, *39*, 3694.
21. Rajeswaran, W.; Cao, Y.; Huang, X.; Wroblewski, E.; Colclough, T.; Lee, S.; Liu, F.; Nagy, P.; Ellis, J.; Levine, B.; Nocka, K.; Messer, W. *J. Med. Chem.* **2001**, *44*, 4563.
22. Glase, S. A.; Akunne, H. C.; Heffner, T. G.; Jaen, J. C.; MacKenzie, R. G.; Meltzer, L. T.; Pugsley, T. A.; Smith, S. J.; Wise, L. D. *J. Med. Chem.* **1996**, *39*, 3179.
23. Yoon, K.; Wilson, T.; Williams, S.; Redda, K. *Drugs Exp. Clin. Res.* **2000**, *26*, 73.
24. Singer, T. P.; Salach, J. I.; Castagnoli, N., Jr.; Trevor, A. *Biochem. J.* **1986**, *235*, 785.
25. Manral, L.; Gupta, P. K.; Suryanarayana, M. V. S.; Ganesan, K.; Malhotra, R. C. *J. Thermal. Anal. Calorimetry* **2009**, *96*, 531.
26. Wichitnithad, W.; McManus, T. J.; Callery, P. S. *Rapid Commun. Mass Spectrom.* **2010**, *24*, 2547.
27. Mabic, S.; Rimoldi, J. M.; Castagnoli, N., Jr. *J. Label. Comp. Radiopharm.* **1997**, *39*, 409.
28. Weissbach, H.; Smith, T. E.; Daly, J. W.; Witkop, B.; Udenfriend, S. *J. Biol. Chem.* **1960**, *235*, 1160.
29. Cheng, Y. C.; Prusoff, W. H. *Biochem. Pharmacol.* **1973**, *22*, 3099.
30. Castagnoli, N., Jr.; Rimoldi, J. M.; Bloomquist, J.; Castagnoli, K. P. *Chem. Res. Toxicol.* **1997**, *10*, 924.
31. Salach, J. I.; Singer, T. P.; Castagnoli, N., Jr.; Trevor, A. *Biochem. Biophys. Res. Commun.* **1984**, *125*, 831.
32. Kitz, R.; Wilson, I. B. *J. Biol. Chem.* **1962**, *237*, 3245.
33. Silverman, R. B.; Yamasaki, R. B. *Biochemistry* **1984**, *23*, 1322.
34. Ungar, F.; Alivisatos, S. G. *Res. Commun. Chem. Pathol. Pharmacol.* **1976**, *13*, 449.
35. Cesura, A. M.; Muggli-Maniglio, D.; Lang, G.; Imhof, R.; Da Prada, M. *J. Neural. Transm. Suppl.* **1990**, *32*, 165.
36. Milczek, E. M.; Bonivento, D.; Binda, C.; Mattevi, A.; McDonald, I. A.; Edmondson, D. E. *J. Med. Chem.* **2008**, *51*, 8019.
37. Ma, J.; Yoshimura, M.; Yamashita, E.; Nakagawa, A.; Ito, A.; Tsukihara, T. *J. Mol. Biol.* **2004**, *338*, 103.
38. Morrison, J. F.; Walsh, C. T. *Adv. Enzymol. Relat. Areas Mol. Biol.* **1988**, *61*, 201.
39. Kinemuchi, H.; Arai, Y.; Oreland, L.; Tipton, K. F.; Fowler, C. J. *Biochem. Pharmacol.* **1982**, *31*, 959.
40. Anderson, M. C.; Waldmeier, P. C.; Tipton, K. F. *Biochem. Pharmacol.* **1991**, *41*, 1871.
41. Holt, A.; Baker, G. B. *NaunynSchmiedebergs Arch. Pharmacol.* **1996**, *354*, 17.
42. Silverman, R. B.; Hiebert, C. K.; Vazquez, M. L. *J. Biol. Chem.* **1985**, *260*, 14648.
43. Fuller, R. W.; Hemrick-Luecke, S. K. *J. Pharm. Exp. Ther.* **1985**, *232*, 696.
44. Hiebert, C. K.; Sayre, L. M.; Silverman, R. B. *J. Biol. Chem.* **1989**, *264*, 21516.
45. Anderson, M. C.; Hasan, F.; McCrodden, J. M.; Tipton, K. F. *Neurochem Res.* **1993**, *18*, 1145.
46. Efange, S. M. N.; Michelson, R. H.; Remmel, R. P.; Boudreau, R. J.; Dutta, A. K.; Freshler, A. *J. Med. Chem.* **1990**, *33*, 3133.
47. Cui, L.; Sapagovas, V.; Lattermann, G. *Liquid Crystals* **2002**, *29*, 1121.
48. Ablordeppey, S. Y.; Fischer, J. B.; Burke Howie, K. J.; Glennon, R. A. *Med. Chem. Res.* **1992**, *2*, 368.
49. Takemura, S.; Miki, Y.; Uono, M.; Yoshimura, K.; Kuroda, M.; Suzuki, A. *Chem. Pharm. Bull.* **1981**, *10*, 3026.
50. Iorio, M. A.; Ciuffa, P.; Damia, G. *Tetrahedron* **1970**, *26*, 5519.
51. Horrillo-Martinez, P.; Hultzsch, K. C.; Gil, A.; Branchadell, V. *Eur. J. Org. Chem.* **2007**, 3311.
52. Rui-Bin, S.; Jin, L.; Xin, L.; Bo-Yi, Q. *ActaPharmacol. Sin.* **2001**, *22*, 639.
53. O'Callaghan, J. P.; Miller, D. B.; Reinhard, J. F., Jr. *Brain Res.* **1990**, *521*, 73.
54. O'Callaghan, J. P. *Neurotoxicol. Teratol.* **1991**, *13*, 275.
55. O'Callaghan, J. P. In *Current Protocols in Toxicology*; Costa, L. G., Ed.; John Wiley & Sons: New York, 2002; pp 12.8.11–12.8.12.
56. Sriram, K.; Benkovic, S. A.; Hebert, M. A.; Miller, D. B.; O'Callaghan, J. P. *J. Biol. Chem.* **2004**, *279*, 19936.